A THEORETICAL STUDY ON THE ACOUSTICALLY DRIVEN OSCILLATING FLOW AROUND SMALL SPHERICAL PARTICLES

Man Yeong Ha*

(Received October 7, 1991)

In order to study the oscillating flow induced by a high intensity acoustic field, a computer code which employs the two-dimensional, unsteady mass and momentum conservation equations for laminar flow in spherical coordinates has been developed. The displacement amplitude of the incident sound wave is large compared to the characteristic length of particles, and the acoustic Reynolds number based on the particle diameter and the velocity amplitude of the oscillating flow is less than about 100. Numerical solutions of these equations give the velocity field, axial pressure gradient, shear stress and flow separation angle around the particle for acoustically oscillating flow as a function of acoustic Reynolds number and Strouhal number. The axial pressure gradient, shear stress and separation angle are proportional to the magnitude of oscillating flow at low frequency (~50Hz) and can be approximated by the quasi-steady analysis. The effects of flow oscillation increase with increasing frequency (~2000Hz) due to combined effects of curvature and flow acceleration, giving different values of axial pressure gradient, shear stress and separation angle for different frequencies of 500, 1000 and 2000 Hz.

Key Words: High Intensity Acoustic Fields, Oscillating Flow, Particles, Flow Separation, Pressure Gradient

NOMENCLATURE

dB	: Decibel
f	: Frequency
L_p	: Sound pressure level
P	: Pressure
Pr	: Prandtl number
r	: Radial position
R	: Radius of particle
R	: Gas constant, Equation(6)
Re_0	: Reynolds number based on steady velocity U_0 (U_0D/ν)
Re_1	: Acoustic Reynolds number(U_1D/ν)
S	: Strouhal number
S_ϕ	: Source term for general variable ϕ
SPL	: Sound pressure level
t	: Time
T	: Period
u_r	: Radial velocity
u_θ	: Axial velocity
U_0	: Steady slip velocity
U_1	: Acoustic peak velocity

Greek symbols

β	: Angular direction defined in the streamwise direction
γ	: Specific heat
Γ_ϕ	: Diffusivity for general variable ϕ
ε_ϕ	: Convergence criteria
θ	: Angular direction
μ	: Viscosity
ρ_g	: Gas density
τ	: Dimensionless time(tf or t/T)
τ_ω	: Shear stress
ϕ	: General variable given in Table 1
ω	: Angular frequency
∞	: Infinity

Subscripts

g	: Gas
new	: New values
old	: Old values
p	: Particle
r	: Radial
s	: Separation
0	: Initial
1	: Acoustic
θ	: Angular
ϕ	: Dependent variables
∞	: Infinity

*Department of Mechanical and Prodution Engineering, Research Institute of Mechanical Technology, Pusan National University, Kumjung Ku, Pusan 609-735, Korea

1. INTRODUCTION

For the steady flow past a solid or fluid sphere at low to moderate Reynolds number, the numerical solutions using a semi-analytical method were obtained by Dennis & Walker (1971) and Oliver & Chung (1987) for the Reynolds numbers in the range 0.1 to 40 and 0.5 to 50, respectively. These studies showed the flow structure and the drag coefficients, and compared their results with those obtained from the previous experimental and theoretical investigations. Oliver & Chung (1987) also studied the internal circulation of a fluid sphere for different Reynolds numbers. Fornberg (1988) obtained numerical solutions for steady viscous flow past a sphere at

high Reynolds number up to 5000. This study calculated the drag coefficients and described the evolution of the wake bubble resembling a Hill's spherical vortex.

Ockendon(1968) and Sano(1981) investigated the unsteady viscous incompressible flow past a sphere when a finite rectilinear velocity is suddenly imparted to the sphere. From the asymptotic solution for small Reynolds number, they calculated the drag coefficient up to the term of $O(Re^2 \ln Re)$. Andres and Ingard (1953 A, B) investigated the acoustic streaming past a sphere. At a high acoustic Reynolds number (order of several hundred) they used the boundary layer equations, and at a low acoustic Reynolds number (order of ten) the Oseen approximation for the solution of the Navier-Stokes equation has been adopted. Here the acoustic Reynolds number is based on the particle diameter and the peak velocity of the oscillating flow. Pozrikidis (1989) considered the problem of viscous oscillating flow past a particle with the unsteady Stokes equation at low acoustic Reynolds numbers. The results obtained by using the boundary-integral method showed the distribution of shear stress on the surface of the sphere with the information of its phase, and described the generation, expansion, and disappearance of an unsteady viscous eddy from a curved boundary for different frequencies.

The studies related to unsteady heat and mass transfer and combustion over a single solid particle, droplet or droplets in the presence of an oscillating acoustic field with and without a steady convective velocity component for various frequency ranges have been an interesting topic of experimental and theoretical investigations (Mori et al., 1969, Larsen & Jensen, 1978, Rawson, 1988, Zinn et al., 1982, Zinn, 1984, Rudinger, 1975, Faeser, 1984, Koopmann et al., 1989, Ha, 1990, Ha & Kim, 1991). These results show varying degree of changes in heat and mass transfer, depending on the frequency and the magnitude of the steady and oscillating flow. They also indicated that the imposed slip velocity between the gas flow and the liquid or solid fuel increases the rate of diffusion of oxidant molecules and the rate of convective heat transfer due to the presence of acoustic oscillations, which results in the enhanced combustion.

The previous studies of oscillating flow past a particle are generally concentrated on the case that the maximum excursion of particles over one period of the flow is small compared to the characteristic size of the particles. However, when the high intensity acoustic fields are applied for the enhancement of combustion and heat and mass transfer to and from particles, the maximum excursion is large compared to the characteristic size of particles. In this case the acoustic Reynolds number is very high compared to the Stoke's flow regime, but it is very low for boundary layer assumptions to be valid, requiring the solution of full Navier-Stokes equations. There have been no detailed theoretical studies investigating the fundamental aspects of this problem in order to understand the governing mechanisms. One reason for this is the enormous computational time. The flow field created by the acoustic field is unsteady and in some cases contain the very high frequency. In order to capture the effects of high frequency a very short time step is needed in the numerical calculations. The main objective of the present paper is to investigate the oscillating flow past solid and droplet fuels such as pulverized coal and coal-water slurry fuels. The numerical solutions of the two-dimensional laminar, unsteady mass and momentum conservation equations are solved for the flow field over a spherical particle exposed to an oscillating acoustic velocity, $U_1 \cos 2\pi ft$. The effects of varying acoustic Reynolds number and Strouhal number on the flow structure, axial pressure gradient, shear stress and flow separation on the surface of particles are discussed in details.

2. GOVERNING EQUATIONS AND BOUNDARY CONDITIONS

The hydrodynamic characteristics of an oscillating flow created by an acoustic field over a single particle are studied by solving the unsteady and two-dimensional axisymmetric conservation equations for constant property, laminar flow with the following common form (see Patankar, 1980) :

$$\frac{\partial}{\partial t}(\rho\phi)+\frac{1}{r^2}\frac{\partial}{\partial r}(r^2\rho u_r\phi)+\frac{1}{r\sin\theta}\frac{\partial}{\partial\theta}(\sin\theta\rho u_\theta\phi)$$
$$=\frac{1}{r^2}\frac{\partial}{\partial r}\left(\Gamma_\phi r^2\frac{\partial\phi}{\partial\tau}\right)+\frac{1}{r^2\sin\theta}\frac{\partial}{\partial\theta}\left(\Gamma_\phi\sin\theta\frac{\partial\phi}{\partial\theta}\right)+S_\phi \quad (1)$$

The flow field and the particle geometry with some nomenclature are shown in Fig. 1. In the conservation of momentum equation, $\phi=u_r, u_\theta$ represents the velocities in the radial r and axial θ directions, respectively. The source terms S_ϕ in Eq. (1) are given in Table 1. The quantities are allowed to vary in the radial (r) and axial (θ) directions whereas a circumferential symmetry is assumed around an axis which passes through the center of the particle and is parallel to the flow direction.

The governing Eq. (1) has the following initial and boundary conditions :

Initial conditions ($t=0$) :

$$\phi=\phi_0 \quad (2)$$

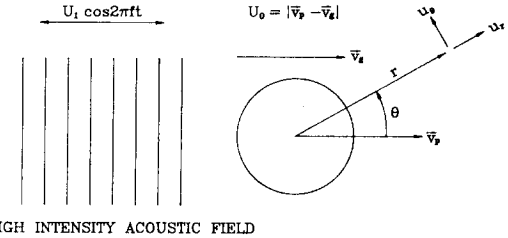

Fig. 1 Schematic diagram showing the geometry and some of the nomenclature used to simulate oscillating flows past a spherical particle in the presence of a high intensity acoustic field

Table 1 Source terms S_ϕ in equation(1)

ϕ	Γ_ϕ	S_ϕ
u_r	μ	$-\frac{\partial p}{\partial r}+\frac{1}{r^2}\frac{\partial}{\partial r}\left(\mu r^2\frac{\partial u_r}{\partial r}\right)+\frac{1}{r\sin\theta}\frac{\partial}{\partial\theta}\left(\mu\sin\theta\frac{\partial u_\theta}{\partial r}\right)$ $-\frac{1}{r^2\sin\theta}\frac{\partial}{\partial r}(\mu\sin\theta u_\theta)-\frac{2\mu}{r^2}\frac{\partial u_\theta}{\partial\theta}-4\mu\frac{u_r}{r^2}$ $-2\mu\frac{u_\theta\cot\theta}{r^2}+\rho\frac{u_\theta}{r^2}$
u_θ	μ	$\frac{1}{r}\frac{\partial P}{\partial\theta}+\frac{1}{r^2}\frac{\partial}{\partial r}\left(\mu r^2\frac{\partial u_\theta}{\partial r}\right)+\frac{1}{r^2\sin\theta}\frac{\partial}{\partial\theta}\left(\mu\sin\theta\frac{\partial u_\theta}{\partial\theta}\right)$ $+\frac{2}{r\sin\theta}\frac{\partial}{\partial\theta}(\mu\sin\theta\frac{u_r}{r})+\frac{\mu}{r}\frac{\partial u_\theta}{\partial r}+\frac{\mu}{r^2}\frac{\partial u_r}{\partial\theta}-\mu\frac{u_\theta}{r^2}$ $-2\mu\frac{u_r\cot\theta}{r^2}-2\mu\frac{u_\theta\cot^2\theta}{r^2}-\frac{1}{r^2}\frac{\partial}{\partial r}(\mu r u_\theta)-\rho\frac{u_r u_\theta}{r^2}$

Boundary conditions ($t>0$) :

$$\frac{\partial \phi}{\partial \theta}=0, \quad at \quad \theta=0 \text{ and } \pi \text{ (Symmetry Conditions)} \tag{3}$$

$$\phi=\phi_p, \quad at \quad r=R \tag{4}$$

and as $r\to\infty$,

$$u_\theta=-U_1\cos(2\pi ft)\sin(\theta)$$
$$u_r=U_1\cos(2\pi ft)\cos(\theta) \tag{5}$$

In Eqs (4) and (5), ϕ_p represents the value of the dependent variable ϕ at the particle surface. In a traveling wave acosutic field with a sound pressure level of P_{rms} and acoustic impedance $\rho_g c$, where ρ_g is the density and $c(=\sqrt{\gamma R T_g})$ is the speed of sound, the peak value of acoustic velocity U_1 is given by

$$U_1=\frac{\sqrt{2}P_{rms}}{\rho_g(\gamma R T_g)^{0.5}} \tag{6}$$

where

$$P_{rmms}=10^A \tag{7}$$

$$A=\frac{L_p-94}{20} \tag{8}$$

where L_p represents the sound pressure level, and the units of L_p and P_{rms} are dB and N/m^2, respectively. The velocities u_{rp} and $u_{\theta p}$ in Eq. (4) at the particle surface are zero.

The numerical solutions of the Eq. (1), using the above initial and boundary conditions, give the velocity fields for oscillating flow over a spherical particle as a function of time. The wall shear stress τ_ω is calculated from the velocity profile as follows :

$$\tau_\omega=\mu\left[r\frac{\partial}{\partial r}\left(\frac{u_\theta}{r}\right)+\frac{1}{r}\frac{\partial u_r}{\partial \theta}\right]_{r=R} \tag{9}$$

The important nondimensional parameters in the present calculation are :

Re_0 : Reynolds number based on steady slip velocity U_0

$S(=fD/U_1)$: Strouhal number

The conservation equations given by Eq. (1) for a single particle are solved using a finite difference method with 30 grids points in the θ, and 50 in the r direction as shown in Fig. 2. The present numberical solution technique for Eq. (1) is the SIMPLEC algorithm of Van Doormaal and Raithby (1982). During the SIMPLEC iteration procedure, the convergence criteria used for ε_ϕ are defined as follows :

$$\varepsilon_\phi=\sum\left|\frac{\phi_{new}-\phi_{old}}{\phi_{new}}\right| \tag{10}$$

where ϕ_{old} represents the values of the previous iteration and ϕ_{new} the updated values from the present iteration for u_r and u_θ.

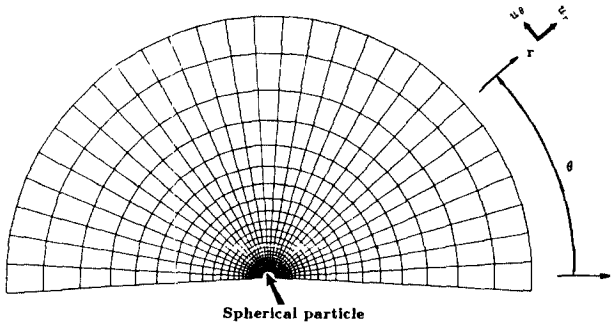

Fig. 2 Coordinate system and computational gird used in the solution of finite difference equations

2. RESULTS AND DISCUSSION

In the present simulation, the particle diameter is fixed at 100 μm in order to consider the flow field over small spherical particles such as pulverized coal particles and coal-water slurry droplets. The numerical solution domain is chosen to be 20 times the particle diameter. The amplitude of the oscillating velocity (U_1) and the frequency (f) of the applied acoustic field are varied in order to investigate the effects of acoustic Reynolds and Strouhal numbers. One period or cycle is divided into 40 uniform time intervals, so that $\delta t=1/40f$ is used as a numerical time stip. A value of 0.005 is used for ε_ϕ in Eq. (10) as a convergence criterion in the present simulation.

For steady flow (without an oscillating flow), the magnitude of the favorable and adverse pressure gradients depends on the magnitude of the steady velocity U_0, increasing with increasing values of U_0. The separation of the steady flow over a sphere starts at a steady Reynolds number of around 20, and the separation angle and the vortex size in the wake region increase with increasing Reynolds number as shown by Clift et al. (1978) due to the increased adverse pressure gradient. Fig. 3 shows a comparison of the separation angle β_s(measured in degrees) from the front stagnation point, obtained from the present simulation, with the approximate correlation given by Clift et al. (1978),obtained from the numerical and experimental results for the steady Reynolds number range of 10 to 400(without a superposed oscillating velocity, $Re_1=0$). As shown in Fig. 3, the present results for the separation angle β_s represent well the correlation given by Clift et al. (1978).

After the successful test runs with steady flows, the program was run for the case of an oscillating flow around a stationary spherical particle. Figs.4 and 5 show the velocity

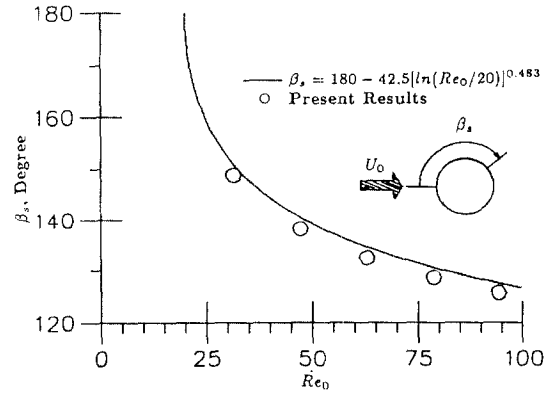

Fig. 3 Comparison of separation angle (β_s) obtained form the present simulation with previous numerical and experimental results

vectors in the domain from R to 2.1R for $Re_0=0.0$ and $Re_1=15.7$ ($U_1=2.5$m/s) corresponding to $S=0.002$(f=50Hz) and S=0.08(f=2000Hz). For these small values of the Strouhal number(0.002 and 0.08) the velocity field reaches quasi-steady state after 4 cycles. Thus the following discussion concentrates on the results over one cycle after reaching a quasi-steady state, unless it is mentioned otherwise.

For the case of the low frequency of 50 Hz (S =0.002), we cannot observe any flow separation (no wake) for $Re_1=15.7$ as shown in Fig. 4. However, if the frequency is increased to 2000 Hz(S=0.08), we can observe the flow separation and formation of a wake even if the acoustic Reynolds number Re_1 based on the amplitude of acoustic velocity, U_1, is lower than 20. In unsteady flow unlike steady flow, the flow field, separation angle, pressure distribution and shear stress on the sphere surface is affected by not only the curvature but the flow acceleration term, $\frac{d\vec{v}}{dt}$. The normalized oscillating flow velocity, U/U_1, and the acceleration, $\frac{1}{2\pi fU_1}\frac{dU}{dt}$, are shown in Fig. 6. The positive sign for U/U_1 during $\tau=0.0\sim0.25$ and $0.75\sim1.0$ represents a flow direction from left to right and the negative sign during $\tau=0.25\sim0.75$ respresents a flow direction from right to left, where τ represents dimensionless time (ft or t/T). The axial pressure gradient, $\frac{1}{r}\frac{\partial P}{\partial\theta}$, due to flow acceleration in the potential flow is expressed as

$$\left(\frac{1}{r}\frac{\partial P}{\partial\theta}\right)_\infty=-2\pi f\rho U_1\sin(2\pi ft)\sin\theta \qquad (11)$$

If we define a new angle β measured from the front stagna-

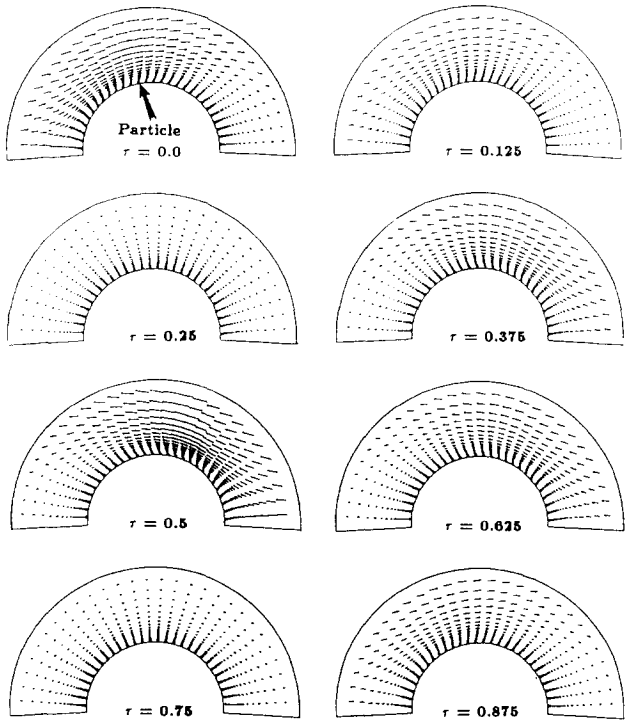

Fig. 4 Velcoity vectors due to an acoustic field with SPL=151 dB and $f=50$ Hz around a spherical particle of diameter 100μm at different times during one cycle : $Re_0=0.0$(no steady flow), $Re_1=15.7$, $S=0.002$

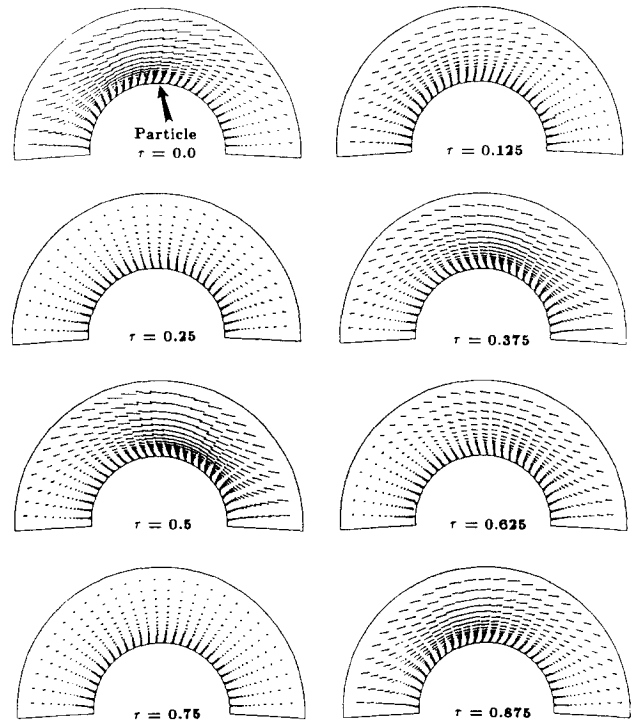

Fig. 5 Velocity vectors due to an acoustic field with SPL=151 dB and f=2000Hz around a spherical particle of diameter 100μm at different times during one cycle: $Re_0=0.0$(no steady flow), $Re_1=15.7$, $S=0.08$

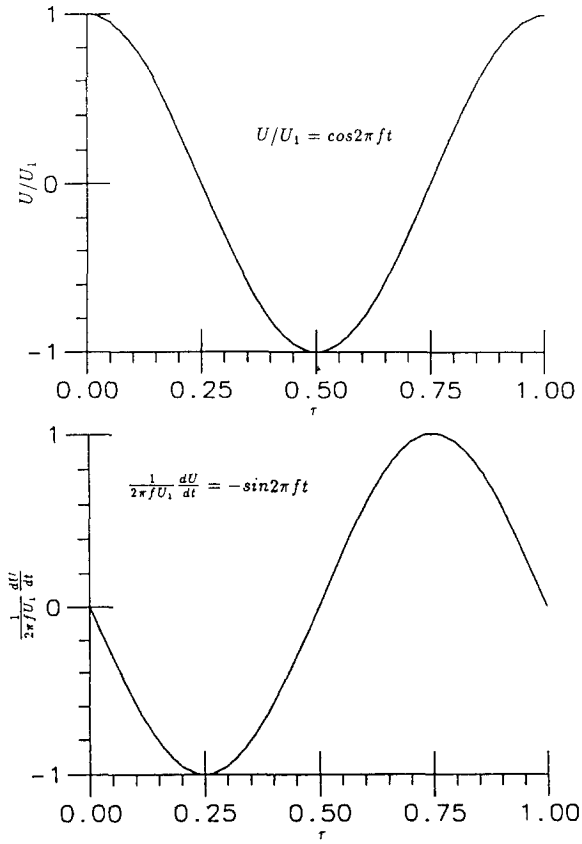

Fig. 6 Normalized oscillating flow velcoity, U/U_1, and the flow acceleration, $\frac{1}{2\pi fU_1}\frac{dU}{dt}$, in the presence of an acoustic field

Table 2 Summary of flow direction and axial pressure gradient for an oscillating flow

τ	0~0.25	0.25~0.5	0.5~0.75	0.75~1.0
Flow Direction	→	←	←	→
Angular Direction	$\beta=\pi-\theta$	$\beta=\theta$	$\beta=\theta$	$\beta=\pi-\theta$
$\frac{dU}{dt}$	<0	<0	>0	>0
$\left(\frac{1}{r}\frac{\partial P}{\partial\theta}\right)_\infty$	APG	FPG	APG	FPG
$\left(\frac{1}{r}\frac{\partial P}{\partial\theta}\right)_\omega>0$	FPG	APG	APG	FPG
$\left(\frac{1}{r}\frac{\partial P}{\partial\theta}\right)_\omega<0$	APG	FPG	FPG	APG

→ : Flow from left to right

← : Flow from right to left

APG : Adverse pressure gradient

FPG : Favorable pressure gradient

$\frac{dU}{dt}$: Acceleration of the oscillating flow velocity U

$\left(\frac{1}{r}\frac{\partial P}{\partial\theta}\right)_\infty$: Axial pressure gradient at infinity (potential flow)

$\left(\frac{1}{r}\frac{\partial P}{\partial\theta}\right)_\omega$: Axial pressure gradient on the surface

tion point (stream-wise direction), this angle is related to the present angular coordinate θ shown in Fig. 1 as follows: at $0.0<\tau<0.25$ and $0.75<\tau<1.0$,

$$\beta=\pi-\theta \tag{12}$$

and, at $0.25<\tau<0,75$,

$$\beta=\theta \tag{13}$$

Using Eqs (12) and (13), Eq. (11) can be rewritten as at $0.0<\tau<0.25$ and $0.75<\tau<1.0$,

$$\left(\frac{1}{r}\frac{\partial P}{\partial\beta}\right)_\infty=2\pi f\rho U_1\sin(2\pi ft)\sin\beta \tag{14}$$

and, at $0.25<\tau<0.75$,

$$\left(\frac{1}{r}\frac{\partial P}{\partial\beta}\right)_\infty=-2\pi f\rho U_1\sin(2\pi ft)\sin\beta \tag{15}$$

Table 2 shows a summary on the flow direction, acceleration and pressure gradient at the infinity due to imposed oscillating flow.

The axial pressure gradient, $\left(\frac{1}{r}\frac{\partial P}{\partial\theta}\right)_\omega$, and shear stress, τ_ω, on the sphere surface are shown in Figs. 7 and 8, respectively, during the half cycle ($\tau=0.0\sim0.5$) for frequencies of 50 Hz ($S=0.002$) and 2000 Hz($S=0.08$). At $\tau=0.0$, the axial pressure gradient due to the flow acceleration of the oscillating flow is 0.0 for both frequencies of 50 and 2000 Hz, as given by Eq. (11) and Table 2. Thus, the curvature effects and the magnitude of the oscillating flow velocity U(=2.5m/s) are the major factors influencing the axial pressure gradient on the sphere surface. The adverse pressure gradient in the downstream region at $\tau=0.0$ is not strong enough to result in flow separation and to form a wake. Thus, the shear stress on the sphere surface has negative values in the stream-wise direction (left to right) for both frequencies of 50 and 2000 Hz, as shown in Fig. 8. At $\tau=0.125$, the axial pressure gradient $\left(\frac{1}{r}\frac{\partial P}{\partial\beta}\right)_\infty$ due to the flow acceleration given by Eq. (14) has positive values resulting in an adverse pressure gradient in the stream-wise direction. The axial pressure gradient is a sine function of the angular coordinate θ, with maximum values of $645N/m^3$ at 50 Hz and $25800N/m^3$ at 2000 Hz at $\theta=\pi/2$. At the low frequency of 50 Hz, the axial pressure gradient (varing in the range 0-$645N/m^3$) due to the flow acceleration is very small and has no effect on the axial pressure gradient on the sphere surface. Thus, the axial pressure gradient depends mainly on curvature and the magnitude of the flow velocity U(=1.768m/s). This results in a lower axial pressure gradient and shear stress, compared to those at $\tau=0.0$, due to a decrease in the flow velocity U (from 2.5 to 1.768m/s). However, if the frequency is increased to 2000Hz, the adverse pressure gradient (varying in the range

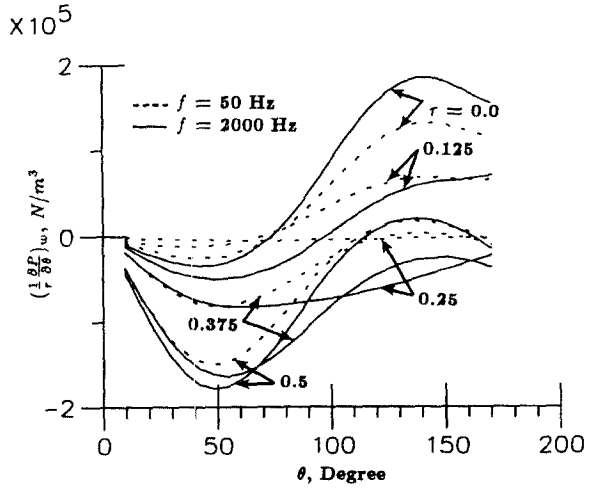

Fig. 7 Axial pressure gradient on the surface during the half cycle ($\tau=0.0\sim0.5$) for frequencies of 50 Hz($S=0.002$) and 2000 Hz($S=0.08$) : $Re_0=0.0$(no steady flow), $Re_1=15.7$(SPL=151dB)

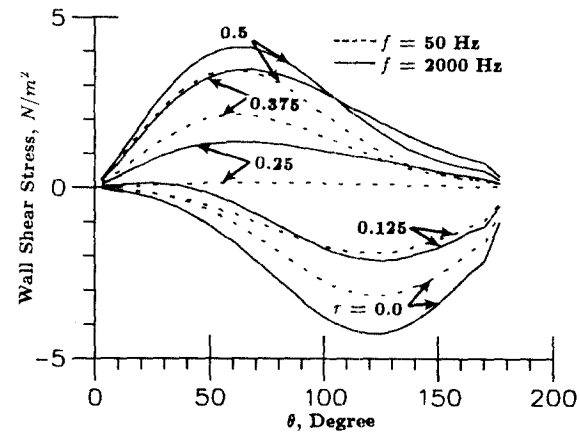

Fig. 8 Shear stress on the surface during the half cycle($\tau=0.0\sim0.5$) for frequencies of 50 Hz($S=0.002$) and 2000 Hz($S=0.08$) : $Re_0=0.0$(no steady flow), $Re_1=15.7$(SPL =151 dB)

0-25800N/m^3) due to the flow acceleration at infinity is 40 times larger than that at 50 Hz. This is a large enough value to affect the axial pressure gradient on the surface. As a result, the magnitude of favorable pressure gradient (positive values of $\left(\frac{1}{r}\frac{\partial P}{\partial \theta}\right)_\omega$) is decreased and the adverse pressure gradient (negative values of $\left(\frac{1}{r}\frac{\partial P}{\partial \theta}\right)_\omega$) is increased, compared to that at 50 Hz as shown in Fig. 7. The adverse pressure gradient at $\tau=0.125$ is larger than that at $\tau=0.0$, even though the flow velocity U decreases, resulting in flow separation. Therefore, the adverse pressure gradient on the surface is affected both by the flow acceleration and by the magnitdue of velocity $U(=1.768\text{m/s})$. Due to flow separation, the shear stress has a zero value at $\theta=40.5$(or $\beta=139.5$) which is defined as the separation point. The shear stress at 2000 Hz, although very small, has positive values for $0.0<\theta<40.5$(separated region) and negative ones for $40.5<\theta<180.0$ whereas that at 50 Hz always has negative values.

Figure.9. shows the axial pressure gradient and shear stress on the sphere surface during the time interval from $\tau=0.125$ to 0.25 in order to indicate clearly the effect of flow acceleration at high frequency. At 2000 Hz, when τ increases from 0.125 to 0.25, the oscillating flow velocity U decreases but the magnitude of the flow acceleration increases, as shown in Fig. 6. Therefore, it is expected that the effect of flow acceleration will increase whereas the effect of curvature and the magnitude of the flow velocity U on the axial pressure gradient and the shear stress on the sphere surface at 2000 Hz will decrease. However, at 50 Hz, the flow acceleration is very small compared to the value at 2000 Hz, resulting in negligible effect on the axial pressure gradient on the sphere surface. Therefore, at 50 Hz, the axial pressure gradient and shear stress on the surface decrease with decreasing values of the oscillating flow velocity U with no flow separation. However, for the case of 2000 Hz, the flow acceleration increases the magnitude of the adverse pressure gradient, even though the oscillating velocity U decreases from 1.768 to 0.0m/s during $\tau=0,125\sim0.25$. This forms a larger wake and the separation point moves upstream ($\beta_s=180\rightarrow0$), as shown in Fig. 9.

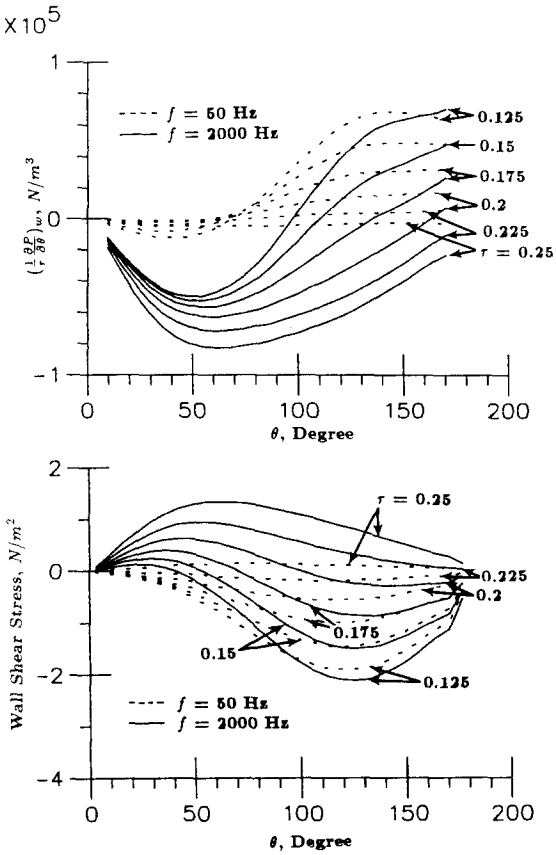

Fig. 9 Axial pressure gradient and shear stress on the surface during $\tau=0.125\sim0.25$ for frequencies of 50 Hz(S=0.002) and 2000Hz(S=0.08) : $Re_0=0.0$(no steady flow), $Re_1=15.7$(SPL=151 dB)

In the following quarter cyle from $\tau=0.25$ to 0.50 and at 50 Hz, curvature effects and the magnitude of the flow velocity U are the major factors affecting the value of the axial pressure gradient and the shear stress on the surface, as in the first quarter cycle between $\tau=0.0$ and 0.25. The flow acceleration has a negligible influence. However, at 2000 Hz, the acceleration (favorable pressure gradient) of the oscillating flow at infinity reaches a maximum at $\tau=0.25$ and a flow can be observed along the surface of the particle from $\theta=0$ to 180, as shown in Figs. 5 and 6, even though the oscillating velocity U is zero. This flow along the surface has the same direction as the oscillating flow U during $\tau=0.25\sim0.5$, increasing the flow velocity compared to that at 50 Hz. At $\tau=0.375$, the axial pressure gradient $\left(\left(\frac{1}{r}\frac{\partial P}{\partial \theta}\right)_\omega\right)$ at 2000 Hz is favorable (negative values) due to the combined effect of the increased flow velocity and the greater flow acceleration with larger values compared to that at 50 Hz, as shown in Fig. 7. This results in no flow separation at $\tau=0.375$, as shown in Figs. 5 and 8, compared to that at $\tau=0.125$, even though the absolute magnitude of oscillating flow velocity U at $\tau=0.375$ is the same as that at $\tau=0.125$, which is 1.768m/s. The shear stress at 2000 Hz is larger than that at 50 Hz due to the increased axial pressure gradient with increasing frequency, as shown in Fig. 8. At $\tau=0.5$, the acceleration of the oscillating flow is zero but the oscillating flow velocity at infinity is at a maximum value of 2.5m/s, as shown in Fig. 6. The axial pressure gradient and shear stress at this time depend mainly on curvature which result in the increased favorable pressure gradient at 2000 Hz due to the effect of the added flow formed along the surface of the particle during $\tau=0.0\sim0.25$, compared to the case of 50 Hz.

The velocity and acceleration of the oscillating flow at infinity during $\tau=0.5\sim0.75$ and $\tau=0.75\sim1.0$ are the same in magnitude as those during $\tau=0.0\sim0.25$ and $0.25\sim0.5$, respectively, but with an opposite sign. As discussed by Andres and Ingard (1953 a, b), an acoustic field generates a steady motion (acoustic streaming) over a spherical particle, which is independent of the flow direction of the oscillating flow U. However, the magnitude of this acoustic streaming has small (second order) effects on the flow field. The flow field over the spherical particle depends mainly on the magnitude of the velocity and acceleration of the oscillating flow U. Therefore, the time history of the axial pressure gradient and shear stress on the sphere surface from $\tau=0.5$ to 0.75 is very similar to that from $\tau=0.0$ to 0.25, and that from $\tau=0.75$ to 1.0 is very similar to that from $\tau=0.25$ to 0.5 except that they are anti-symmetric.

At the acoustic Reynolds number of 15.7 and at 50 Hz, the flow acceleration has a secondary effect but the curvature and the absolute magnitude of the oscillating velocity U have

a major effect on the axial pressure gradient on the sphere surface. Therefore, we cannot observe any flow separation in the flow (stream-wise) direction. However, if the frequency is increased to 2000 Hz, the flow acceleration becomes an important factor as well as the curvature effects, inducing flow separation, even if the acoustic Reynolds number Re_1 is less than 20 which is the value of steady Reynolds number at which first wake is observed. Figure 10 shows the variation of the location of the separation point β_s as a function of τ for an acoustic Reynolds number of 15.7 and frequency of 2000 Hz. The circular symbol in Fig. 10 represents the computational results for β_s. The separation point moves upstream ($\beta_s=180\rightarrow0$) with increasing acceleration of the oscillating flow during $\tau=0.0\sim0.25$ and $0.5\sim0.75$, giving a flow along the surface of the particle which has the same direction as the oscillating flow velcoity U in the following cycle from $\tau=0.25$ to 0.5 and 0.75 to 1.0, respectively.

Figures.11 and 12 shows the velocity vectors in the domain from R to 2.1 R for $Re_0=0$ and $Re_1=94.4$ ($U_1=15$m/s) corresponding to $S=0.0003$(f=50Hz) and $S=0.013$(f=2000Hz) over one cycle. During a cycle, the direction of the oscillating flow U, the location of the stagnation point, the flow acceleration and the axial pressure gradient due to the flow acceleration at infinity for $Re_1=94.4$ ($U_1=15$m/s) are similar to the case of $Re_1=15.7$ ($U_1=2.5$m/s). However, since the Re_1 is larger than 20, a wake is formed at both frequencies of 50 and

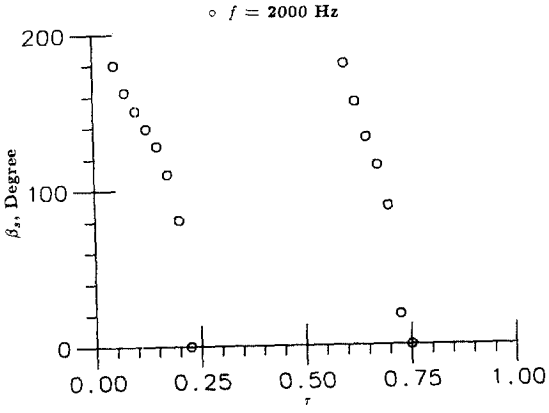

Fig. 10 Variation of the separation angle β_s as a function of τ : $Re_0=0.0$(no steady flow), $Re_1=15.7$(SPL=151dB), $S=0.08$($f=2000$ Hz)

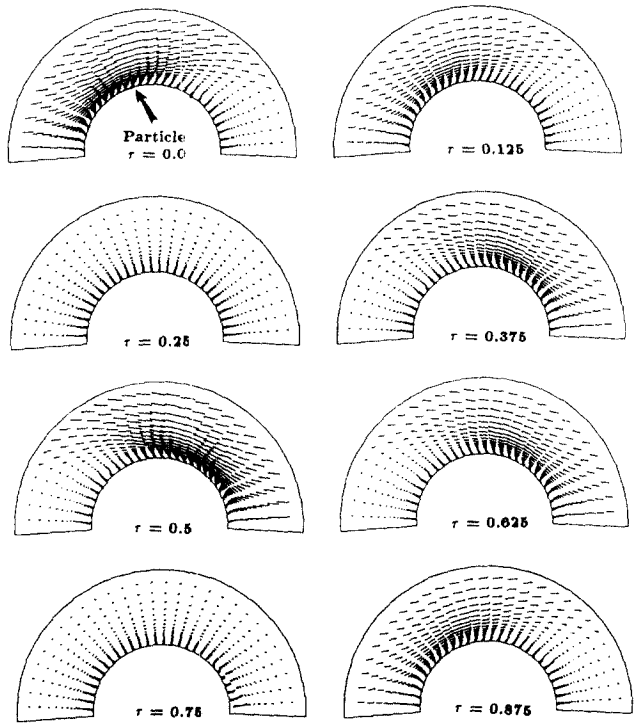

Fig. 11 Velocity vectors due to an acoustic field with SPL=167 dB and $f=50$ Hz around a spherical particle of diameter 100μm at different times during one cycle : $Re_0=0.0$(no steady flow), $Re_1=94.4$, $S=0.00033$

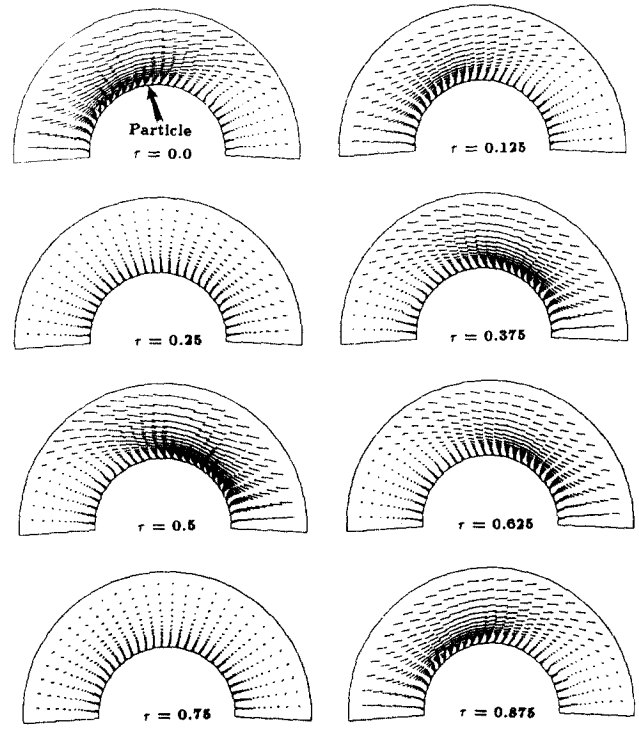

Fig. 12 Velocity vectors due to an acoustic field with SPL=167 dB and $f=2000$ Hz around a spherical particle of diameter 100μm at different times during one cycle : $Re_0=0.0$(no steady flow), $Re_1=94.4$, $S=0.0013$

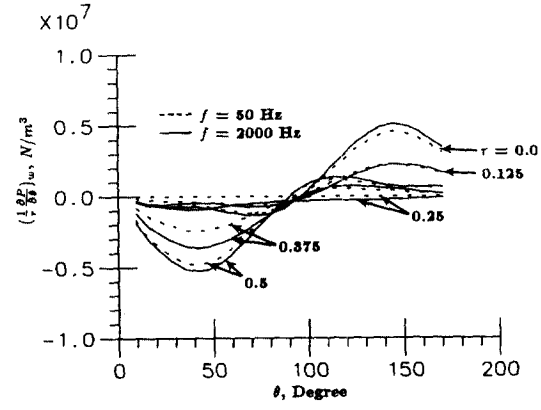

Fig. 13 Axial pressure gradient on the surface during a half cycle ($\tau=0.0\sim0.5$) for frequencies of 50Hz($S=0.00033$) and 2000 Hz($S=0.0013$) : $Re_0=0.0$(no steady flow), $Re_1=94.4$(SPL=167 dB)

2000 Hz and the wake size for 2000 Hz is larger than that at 50 Hz, as shown in these figures.

At the frequency of 50 Hz, the axial pressure gradient due to flow acceleration at infinity for $Re_1=94.4$ is six times larger than that for $Re_1=15.7$ but still too small to affect the axial pressure gradient on the sphere surface. Thus, as in the case of $Re_1=15.7$, the curvature effects and the absolute magnitude of the oscillating flow velocity U become the major influences determining the flow field, separation angle, the axial pressure gradient and the shear stress on the sphere surface. However again at 2000 Hz, the acceleration becomes an important factor in determining the flow field, flow separation, the axial pressure gradient and shear stress on the surface.

Figures.13. and 14 show the axial pressure gradient and shear stress on the sphere surface at frequencies of 50 and 2000 Hz for the acoustic Reynolds number of 94.4 during the half cycle from $\tau=0$ to 0.5. The axial pressure gradient and shear stress on the sphere surface during $\tau=0.125\sim0.25$ is shown in Fig. 15 as a function of τ. The overall trends at $Re_1=94.4$ are similar to the case of $Re_1=15.7$. During the first quarter cycle from $\tau=0.0$ to 0.25, the flow acceleration induces an adverse pressure gradient at infinity with a minimum value at $\tau=0.0$ and maximum at $\tau=0.25$, as hown in Fig. 6 Thus, at 2000 Hz, increasing flow acceleration leads to decrease the favorable pressure gradient (positive values of $\left(\frac{1}{r}\frac{\partial P}{\partial\theta}\right)_\omega$) in the upstream region and increase the adverse pressure gradient (negative values of $\left(\frac{1}{r}\frac{\partial P}{\partial\theta}\right)_\omega$) in the wake at $\tau=0.125$ and 0.25. The shear stress on the sphere surface is proportional to the magnitude of the axial pressure gradient on the sphere surface, resulting in high shear stress for high axial pressure gradient and low shear stress for low axial pressure gradients. Around $\tau=0.25$, the flow from $\theta=0$ to 180 is formed near the surface due to the flow acceleration at 2000 Hz, as shown in Fig. 12, even though the oscillating flow velcoity U is zero. The magnitude of this flow increases with increasing acoustic Reynolds number from 15.7 to 94.4

Similar to the case of $Re_1=15.7$, at 2000 Hz, the flow in the direction $\theta=0$ to 180 formed on the sphere surface during the previous cycle and the acceleration of the oscillating flow have complementary effects on the axial pressure gradient in the quarter cycle from $\tau=0.25$ to 0.5. This results in an increase in the magnitude of the axial pressure gradient along the sphere surface, as shown in Fig. 13.

The axial pressure gradient and shear stress on the sphere surface at dimensionless time from $\tau=0.5$ to 0.75 are very similar to those at time from 0.0 to 0.25, and those from $\tau=0.75$ to 1.0 are very similar to those from 0.25 to 0.5 except that they are anti-symmetric. The reasons for this have been discussed previously.

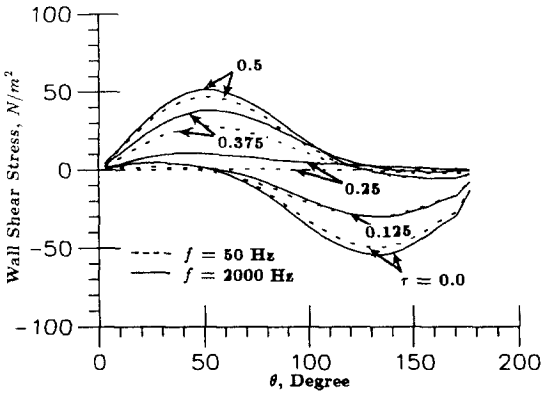

Fig. 14 Shear stress on the surface during the half cycle($\tau=0.0\sim0.5$) for frequencies of 50Hz(S=0.00033) and 2000 Hz(S=0.0013) : $Re_0=0.0$(no steady flow), $Re_1=94.4$(SPL=167 dB)

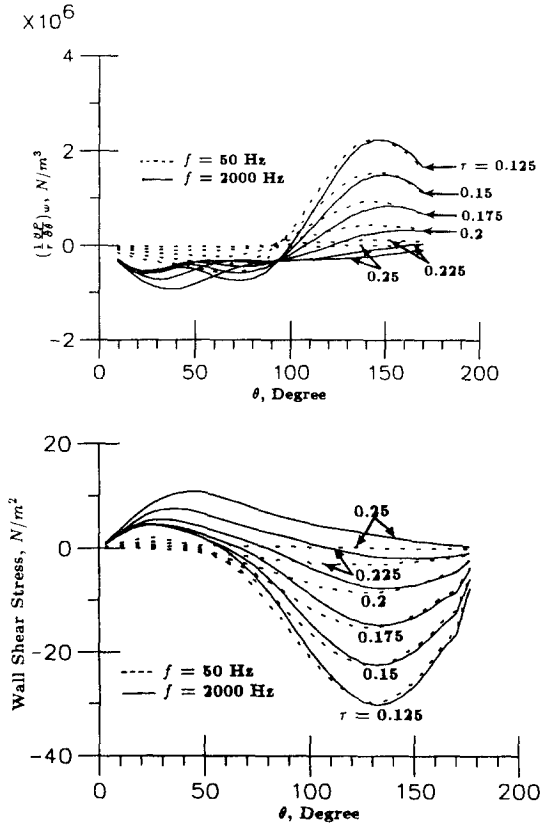

Fig. 15 Axial pressure gradient and shear stress on the surface during $\tau=0.125\sim0.25$ for frequencies of 50Hz(S=0.00033) and 2000Hz(S=0.0013) : $Re_0=0.0$(no steady flow), $Re_1=94.4$(SPL=167 dB)

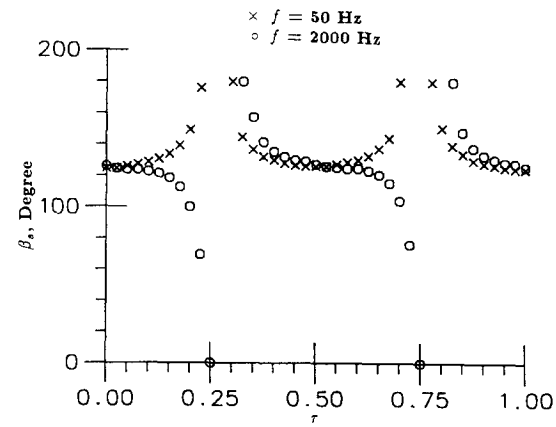

Fig. 16 Variation of the separation angle β_s as a funcition of τ for frequencies of 50 Hz(S=0.00033) and 2000Hz(S=0.0013) : $Re_0=0.0$(no steady flow), $Re_1=94.4$(SPL=167 dB)

Figure 16 shows the separation angle β_s as a function of τ during one cycle for $Re_1=94.4$. With decreasing magnitude of the oscillating velcoity U during $\tau=0.0\sim0.25$ and $\tau=0.5\sim0.75$, the separation point β_s at 50 Hz is moved downstream ($\beta_s=0\rightarrow180$), resulting in a wake decreasing in size. However, at 2000 Hz, the separation point is moved upstream ($\beta_s=180\rightarrow0$) due to the increased effects of flow acceleration (adverse pressure gradient) with increasing wake size. With the increasing magnitude of the oscillating velocity U during $\tau=0.25\sim0.5$ and $\tau=0.75\sim1.0$, the separation point at 50 Hz is moved upstream with increased spread. When the frequency is increased to 2000 Hz, the flow starts to separate later due to the effects of flow acceleration (favorable pressure gradient) during this time period, resulting in the larger values of β_s and a wake decreasing in size compared to the case of 50 Hz.

3. CONCLUSIONS

The axisymmetric, laminar mass and momentum conservation equations for flow around a single spherical particle in the presence of an acoustic field are solved numerically with different values of the acoustic Reynolds number and Strouhal number. In the case of an oscillating flow around a spherical particle, the velocity fields reach the quasi-steady state after four or five cycles for low Strouhal numbers ($S=0.0002\sim0.4$) considered in the present study. Axial pressure gradient, shear stress and flow separation on the particle surface depend on the change of velocity U due to body curvature and flow acceleration. At low frequencies ($\sim$50 Hz), curvature effects are dominant, resulting in increasing values of these values with increasing U. At high frequencies ($\sim$2000 Hz), the effects of flow acceleration increase. The combined effects of curvature and flow acceleration determine the axial pressure gradient, shear stress and flow separation. There is an increase in the size of wake with increasing frequencies even though the flow velocity U decreases.

REFERENCES

Andres, J.M. and Ingard, U., 1953(a), "Acoustic Streaming at High Reynolds Number," J. of the Acoustical Society of America, Vol. 25, pp. 928~932.

Andres, J.M. and Ingard, U., 1953(b), "Acoustic Streaming at Low Reynolds Number," J. of the Acoustical Society of America, Vol. 25, pp. 932~938.

Clift, R., Grace, J.R. and Weber, M.E., 1978, "Bubbles, Drops, and Particles," Academic Press, Inc.

Dennis, S.C.R. and Walker, J.D.A., 1971, "Calculation of the Steady Flow Past a Sphere at Low and Moderate Reynolds Number," J. Fluid Mech, Vol. 48, pp. 771~789.

Faeser, R.J., 1984, "Acoustic Enhancement of Pulverized Coal Combustion," ASME Paper, 84-WA/NCA-18.

Fornberg, B., 1988, "Steady Viscous Flow Past a Sphere at High Reynolds Numbers," J. Fluid Mech., Vol. 190, pp. 471~489.

Ha, M.Y., 1990, "A Theoretical Study of Augmentation of Particle Combustion Via Acoustic Enhancement of Heat and Mass Transfer," Ph.D. Thesis, The Pennsylvania State University.

Ha, M.Y. and Kim, K.C., 1991, "Heat Transfer Past Particles Entrained in an Oscillating Flow with and Without a Steady Velocity," Proceedings of the KSME Spring Annual Meeting '91, pp. 385~390

Koopmann, G.M., Scaroni, A.W., Yavuzkurt, S., Reethof, G., Ramachandran, P. and Ha, M.Y., 1989, "Acoustically Enhanced Combustion of Micronized Coal Water Slurry Fuel," Final Report to DOE/METC under Contract No. DE-RA21-86MC23257.

Larsen, P.S. and Jensen, J.W., 1978, "Evaporation rates of Drops in Forced Convection with Superposed Transverse Sound Field," Int'l. J. Heat and Mass Transfer, Vol. 21, pp. 511~517.

Mori, Y., Imabayashi, M., Hijikata, K. and Yoshida, Y., 1969, "Unsteady Heat and Mass Transfer From Spheres," Int' 1. J. Heat Mass Transfer, Vol. 12, pp. 571~585.

Ockendon, J.R., 1968, "The Unsteady Motion of a Small Sphere in a Viscous Liquid," J. Fluid Mech., Vol. 34, pp. 229~239.

Oliver, D.L.R. and Chung, J.N., 1987, "Flow About a Fluid Sphere at Low to Moderate Reynolds Numbers," J. Fluid Mech., Vol. 177, pp. 1~18.

Patankar, S.V., 1980, "Numerical Heat Transfer and Fluid Flow. Hemisphere," Washington D.C.

Pozrikidis, C., 1989, "A Study of Linearized Oscillatory low Past Particles by the Boundary-Integral Method," J. Fluid Mech., Vol. 202, pp. 17~41.

Rawson, S.A., 1988, "An Experimental Investigation of the Influence of High Intensity Acoustics on Heat and Mass Transfer Rates from Spheres as Related to Coal water Slurry Fuel Combustion Enhancement," M.S. Thesis, The Pennsylvania State University.

Rudinger, G., 1975, "Effect of Velocity Slip on the Burning Rate of Fuel Particles," J. of Fluids Engineering, pp.321~326.

Sano, T., 1981, "Unsteady flow past a sphere at low Reynolds Number," J. fluid Mech., Vol. 112, pp. 433~441.

Van Doormaal, J.P. and Raithby, G.D., 1982, "Enhancement of the SIMPLE Method for Predicting Incompressible Fluid Flow," Numerical Heat Transfer, Vol. 7, pp. 147~163.

Zinn, B.T., Carvalho, Jr., J.A., Miller, N. and Daniel, B.R., 1982, "Pulsating Combution of Coal in a Rijke Type Combustor," 19th Symposium (International) on Combustion, The Combustion Institute, pp. 1197~1203.

Zinn, B.T., 1984, "State of the Art and Research Needs of Pulsating Combustion," ASME Paper, 84-WA/NCA-19.